Biochimica et Biophysica Acta 1850 (2015) 1438–1448

Contents lists available at ScienceDirect

Biochimica et Biophysica Acta

journal homepage: www.elsevier.com/locate/bbagen

Hedgehog signaling through GLI1 and GLI2 is required for epithelial–mesenchymal transition in human trophoblasts

Chao Tang [a], Liu Mei [a], Liyu Pan [a], Wenyi Xiong [b], Haibin Zhu [b], Hongfeng Ruan [a], Chaochun Zou [b], Lanfang Tang [b], Takuma Iguchi [c], Ximei Wu [a,*]

[a] Department of Pharmacology, School of Medicine, Zhejiang University, Hangzhou, China
[b] The Affiliated Children Hospital, School of Medicine, Zhejiang University, Hangzhou, China
[c] Department of Toxicology, Osaka University, Suita, Osaka, Japan

ARTICLE INFO

Article history:
Received 18 October 2014
Received in revised form 31 March 2015
Accepted 8 April 2015
Available online 15 April 2015

Keywords:
Hedgehog signaling
Trophoblast
Epithelial–mesenchymal transition

ABSTRACT

Background: Epithelial to mesenchymal transition (EMT) is critical for human placental development, trophoblastic differentiation, and pregnancy-associated diseases. Here, we investigated the effects of hedgehog (HH) signaling on EMT in human trophoblasts, and further explored the underlying mechanism.
Methods: Human primary cytotrophoblasts and trophoblast-like JEG-3 cells were used as in vitro models. Quantitative real-time RT-PCR and Western blot analysis were performed to examine mRNA and protein levels, respectively. Lentiviruses expressing short hairpin RNA were used to knock down the target genes. Reporter assays and chromatin immunoprecipitation were performed to determine the transactivity. Cell migration, invasion and colony formation were accessed by wound healing, Matrigel-coated transwell, and colony formation assays, respectively.
Results: Activation of HH signaling induced the transdifferentiation of cytotrophoblasts and trophoblast-like JEG-3 cells from epithelial to mesenchymal phenotypes, exhibiting the decreases in E-Cadherin expression as well as the increases in vimentin expression, invasion, migration and colony formation. Knockdown of GLI1 and GLI2 but not GLI3 attenuated HH-induced transdifferentiation, whereas GLI1 was responsible for the expression of HH-induced key EMT regulators including Snail1, Slug, and Twist, and both GLI1 and GLI2 acted directly as transcriptional repressor of *CDH1* gene encoding E-Cadherin.
Conclusion: HH through GLI1 and GLI2 acts as critical signals in supporting the physiological function of mature placenta.
General significance: HH signaling through GLI1 and GLI2 could be required for the maintenance of human pregnancy.

1. Introduction

Hedgehog (HH) signaling has conserved roles in the differentiation of various cells in metazoans ranging from *Drosophila* to humans [1,2]. The mammalian HH ligands consist of sonic hedgehog (SHH), indian hedgehog (IHH) and desert hedgehog (DHH). In vertebrates, in the absence of HH, patched-1 (PTC1) receptor represses smoothened (SMO) activity, and the GLI transcription factors (GLI2 and GLI3) are proteolytically cleaved into their repressors within the primary cilium. In the presence of HH, binding of HH to PTC1 relieves the suppression of SMO, resulting in activation of GLI transcription factors (GLI1, GLI2 and GLI3) and inducing the transcription of the target genes including cyclin D, cyclin E, myc as well as PTC1 and GLI1 [3,4]. Overall, the conserved effect of HH is to switch the GLI transcription factors from repressors into activators and allow for fine-tuned transcriptional events.

Epithelial–mesenchymal transition (EMT) is a process in which epithelial cells lose the polarity and adhesiveness, change into a mesenchymal phenotype and gain the capacity of increased mobility [5]. EMT plays crucial roles in development of multiple tissues and organs, and also contributes to tissue repair and carcinoma progression [6]. In human placental development, trophoblast cells differentiate into either the villous cytotrophoblast (CTB) lineage to form the syncytiotrophoblast (STB) that secretes the majority of placental hormones, or the invasive extravillous cytotrophoblast (EVT) lineage to anchor the chorionic villi in the uterus [7,8]. Invasive EVTs migrate through the endometrium, interact with decidual cells and immunocompetent cells, and differentiate into multinucleated placental bed giant cells. On the other hand, EVTs can invade the maternal spiral arteries, mediate the destruction of the arterial wall, and replace the endothelium, forming endovascular trophoblasts [9,10]. Upon acquisition of migratory ability, EVTs tend to lose their tight epithelial assembly and phenotype, becoming loosely

* Corresponding author at: Department of Pharmacology, School of Medicine, Zhejiang University, No. 688, Yuhangtang Road, Hangzhou 310058, China. Tel./fax: +86 571 8898 1121.
E-mail address: xiwu@zju.edu.cn (X. Wu).

http://dx.doi.org/10.1016/j.bbagen.2015.04.005
0304-4165/

attached, subsequently invading the maternal decidua as interstitial cytotrophoblasts. The process by which placental trophoblasts originate as epithelial cells and are subsequently triggered to change from an epithelial to a mesenchymal-like migratory phenotype, resembling EMT is identified in other developmental processes [7,8].

The link between EMT and HH signaling has been previously established in many pathological conditions. For instance, HH/GLI signals regulate the EMT in pancreatic carcinoma, hepatocellular carcinoma, gastrointestinal neuroendocrine tumors, and lung squamous cell carcinoma [11–13]; and HH signals regulate EMT in renal and biliary fibrosis [14,15]. To date, HH signaling regulating EMT in physiological conditions has not yet been studied. Hence, we investigated the roles of HH signaling in EMT in human primary cytotrophoblasts, and explored the underlying mechanisms in trophoblast-like cells. Our results demonstrate that HH signals stimulate EMT of placental cytotrophoblast possibly by inducing the GLI1-controlled expression of key transcriptional factors of EMT and both GLI1- and GLI2-controlled transcription of a downstream target gene, *CDH1*, encoding E-Cadherin. This work establishes HH signaling as an essential mechanism in maintaining the physiological functions of adult placentas.

2. Materials and methods

2.1. Cell lines

Trophoblast-like JEG-3 cells were obtained from ATCC (Manassas, VA), and cultured in DMEM/F12 = 1:1 medium (Hyclone, USA) supplemented with 10% (v/v) fetal bovine serum (Life Technologies, Inc., Grand Island, NY) at 37 °C with 5% CO_2 as described previously [16,17]. 293 EcR SHH cells (SHH-expressing cells, ATCC) and control HEK 293 cells were used for the production of biologically active murine SHH conditional medium (SM) and control medium (CM), respectively, in the presence of ecdysone [18]. The specificity of SM was confirmed by 5E1 SHH blocking antibody (DSHB, Iowa City, Iowa). 293FT packaging cells (Life Technologies) and GP293 retroviral packaging cells (Clontech Laboratories, Inc., Mountain View, CA) for generating the lentiviruses and retroviruses were cultured as described previously [17,19].

2.2. Isolation and culture of cytotrophoblasts

Human placentas were obtained from uncomplicated normal term (38–40 W) pregnancy after elective cesarean section without labor, following a protocol approved by the Ethics Committee of School of Medicine of Zhejiang University. The primary cytotrophoblasts were isolated and purified as described previously [17]. Briefly, tissue aliquots were removed from the maternal side of the placenta and digested with 0.125% trypsin (Sigma, St. Louis, MO) in DMEM (Life Technologies). The placental cytotrophoblasts were purified using a 5–65% Percoll (Sigma) gradient at step increments of 5%. The cells were plated at a density of 1.5×10^6 cells per well in 6-well plates, and were cultured at 37 °C with 5% CO_2 and 95% air in DMEM containing 10% newborn calf serum (Life Technologies) to allow syncytialization in vitro.

2.3. RNA isolation, RT-PCR and quantitative real-time PCR

Total RNA was isolated from JEG-3 cells and cytotrophoblasts by using a TRIzol reagent (Takara Biotechnology Co., Ltd., Dalian, China) according to the manufacturer's instructions. 5 μg total RNA in a volume of 20 μl was reversely transcribed by using SuperScript III reagent (Life Technologies) and the oligo-(deoxythymidine) primer with incubation at 42 °C for 1 h. After the termination of cDNA synthesis, each reaction mixture was diluted with 80 μl Tris–EDTA buffer. Messenger RNA levels of target genes were determined by RT-PCR and quantitative RT-PCR as described previously [17,20]. The relative amounts of the mRNA levels of the target genes were normalized to the glyceraldehyde-3-phosphate dehydrogenase (GAPDH) levels, respectively, and the relative difference in mRNA levels was calculated by $2^{-\Delta\Delta Ct}$ method [21]. The primers were listed in the Supplementary data (Table S1).

2.4. Western blotting

Total protein extracts were prepared in whole cell lysis buffer (50 mM HEPES, 150 mM NaCl, 1 mM EGTA, 10 mM sodium pyrophosphate, 1.5 mM $MgCl_2$, 100 mM sodium fluoride, 10% glycerol, and 1% Triton X-100) containing an inhibitor mixture (1 mM phenylmethylsulfonyl fluoride, 10 μg/ml aprotinin, and 1 mM sodium orthovanadate). Protein concentrations were determined using a standard Bradford assay, and 50 μg of total protein was subjected to SDS-PAGE followed by a transfer onto PVDF membranes (Millipore, Bedford, MA). Membranes were incubated overnight at 4 °C with primary antibodies against E-Cadherin (SC-7870, Santa Cruz Biotechnology Inc., Santa Cruz, CA), vimentin (SC-6260, Santa Cruz), GLI1 (SC-20687, Santa Cruz), GLI2 (ab26056, Abcam Ltd., Cambridge, UK), GLI3 (ab69838, Abcam), and β-actin (SC-69879, Santa Cruz) followed by incubation in secondary antibodies. Signals were developed using the Enhanced Chemiluminescence System. National Institutes of Health Image software (ImageJ, http://rsb.info.nih.gov/ij/) was used to quantify the immunoreactive bands, and the normalized antigen signals were calculated from target protein-derived and β-actin-derived signals. The mean density of bands from the control cells was set to 1.

2.5. Immunohistochemistry and immunocytochemistry staining

Immunohistochemistry staining was performed by using the Histostain-Plus Kit (Kangwei Reagents, Beijing, China) according to the manufacturer's instructions. Briefly, paraffin-embedded placental sections (4 μm) were deparaffinized and rehydrated in xylene and a graded series of ethanol. After antigen retrieval in 10 mM sodium citrate and 10 mM citric acid, tissue sections were then incubated with 3% H_2O_2 in methanol to quench endogenous peroxidase followed by sequential incubation included with normal serum for 30 min, with control IgG and primary antibodies against SHH (06-1106, Millipore, Billerica, MA), IHH (ab39634, Abcam Ltd., Cambridge, UK), DHH (SC-271168, Santa Cruz), PTC1 (06-1102, Millipore), SMO (ab72130, Abcam), GLI1 (SC-20687, Santa Cruz), GLI2 (ab26056, Abcam Ltd., Cambridge, UK) and GLI3 (ab69838, Abcam) at 4 °C overnight, and with HRP-labeled secondary antibody (Life Technologies) for 30 min. The diaminobenzidine (DAB) solution was used for development of color, and the sections were counterstained with hematoxylin. Immunocytochemistry was performed on chamber slides (Nalge Nunc International, Naperville, IL). Either JEG-3 cells or cytotrophoblasts were fixed in ice-cold methanol and permeabilized with 0.1% Triton X-100 in PBS (PBST). After incubation with blocking buffer (1% bovine serum albumin), the cells were incubated with primary antibodies against E-Cadherin or vimentin. After washing with PBST, the cells were incubated with Alexa 488- or 555-conjugated secondary antibodies (Life Technologies). The nuclei were counterstained with 4′,6-diamidino-2-phenylindole (DAPI). Slides were analyzed by a laser scanning microscope.

2.6. Wound healing, Matrigel invasion and colony formation assays

For wound healing assays, the cells were seeded in 6-well plates (2×10^5 cells/well). After various treatments, the confluent monolayer of cells was scrapped with a sterile tip to create an artificial wound, and then incubated with either CM or SM and allowed to heal. Cell migration to the wounded surface was then monitored by microscopy after 48 h, and the distance between the edges of the wound was measured by Photoshop CS3. Invasion of cells was measured in Matrigel-coated Transwell inserts (6.5 μm, Costar, Cambridge) containing polycarbonate filters with 8-μm pores as detailed previously [22]. After various treatments, JEG-3 cells (2×10^5) in 200 μl of serum-free medium were plated in the upper chamber, whereas 600 μl of medium

with 10% fetal bovine serum was added to the lower well. After incubation for 24 h, non-invaded cells on top of the Transwell were scraped off, and the invaded cells on the other side were washed with PBS and fixed in methanol for 10 min followed by a staining with crystal violet [22]. The invaded cells were counted under a light microscope. For colony formation assays, the cells were seeded in 6 cm plates at a density of 1000 cells/well in 4 ml CM or SM. After culturing for two weeks, colonies were stained with 0.5% crystal violet in 2% ethanol and colonies were counted [23].

2.7. Retroviral overexpression of SMO*, GLI1, ΔN-GLI2 and GLI3-ΔC

Generation of retroviruses expressing target genes was described previously [19]. Briefly, GP293 retroviral packaging cells were maintained in Dulbecco's modified Eagle's medium containing 10% FCS, and were transiently cotransfected with 4 μg of pVSV-G vector (Clontech) plus 5 μg of pLXRN-GLI1, pLXRN-ΔN-GLI2, pLXRN-GLI3-ΔC, pLXRN-YFP (yellow fluorescent protein) or pLXRN-YFP-SMO* by the Lipofectamine 2000 (Life Technologies). After transfection, medium was changed to regular medium, and retrovirus-containing supernatants were harvested 72 h after transfection, virus was concentrated by ultracentrifugation according to the manufacturer's protocol, and the retroviral supernatants with titer more than 1×10^6 CFU/ml were used for infection. JEG-3 cells were exposed to retrovirus containing medium for 24 h in the presence of 6 μg/ml of polybrene (Sigma), and the infection efficiency was determined by YFP-positive cells (more than 80%).

2.8. Generation of lentiviruses expressing GLI1–, GLI2– or GLI3–shRNA

Generation of lentivirus expressing shRNA was described previously [17]. For construction of lentiviral shRNA-expressing vectors, the hairpin shRNA templates of complementary oligonucleotide containing and overhangs were digested. The synthesized complementary oligonucleotides were annealed and inserted into the sites *Xba*I and *Not*I of a lentiviral shRNA expression vector, Pll3.7. The integrity of the shRNA-expressing construct was amplified by a DNA sequencer. The sequences of oligonucleotides were listed in the Supplementary data (Table S2). 293FT packaging cells were transfected with 6 μg of each construct by Lipofectamine 2000 reagents, 72 h after transfection, lentivirus-containing supernatants were harvested, and the titers more than 1×10^6 colony forming U/ml were used for infection in JEG-3 cells for 24 h in the presence of 8 μg/ml polybrene (Sigma).

2.9. Reporter construction, transient transfection and reporter assays

Complex human *E-Cadherin* (*CDH1*, nt −552/+12 and nt −329/+12) and *vimentin* (*VIM*, nt −2488/+250) gene promoter regions were amplified by PCR in the presence of genomic DNA from JEG-3 cells. The PCR products were cloned into pGL3-Basic vector (Promega, Madison, WI) to generate the luciferase reporter constructs of *E-Cadherin* and *vimentin*. The mutation at potential binding sites of GLIs was introduced by site-directed mutagenesis. All of these constructs were verified by a DNA sequencer. Transient transfection was performed by using Lipofectamine 2000 as per the manufacturer's instructions. Briefly, JEG-3 cells were seeded in 24-well culture plates overnight to reach 50–70% before transfection. The cells were transfected for 8 h in the absence of serum. Each well contained 2 μl Lipofectamine 2000 reagents, 2 μg luciferase reporter plasmids, and 0.02 μg pRL-null expressing Renilla luciferase (Promega) with or without 2 μg of constitutively active form of SMO (SMO*), GLI1 or N-terminally truncated GLI2 (ΔN-GLI2). The cells were then either cultured in the normal growth medium for 48 h before harvest or incubated in either CM or SM for 48 h. After the cells were harvested, the cellular lysates were prepared in 100 μl reporter lysis buffer (Promega), and the 20 μl of supernatants was used for dual-luciferase assay according to the manufacturer's instructions (Promega). The firefly luciferase levels were normalized to Renilla luciferase levels.

2.10. Chromatin immunoprecipitation assays

Chromatin immunoprecipitation (ChIP) was conducted using a commercial kit (17-295, Millipore, Billerica, MA) and a method modified from the manufacturer's protocol. Briefly, the cells were fixed with 1% formaldehyde to cross-link the transcription factors to chromatin DNA. After washing with PBS, the cells were re-suspended with lysis buffer supplemented with protease inhibitor cocktail. The shearing of chromatin DNA was performed by sonication to produce an approximately 500 bp of input DNA, and was subjected to immunoprecipitation

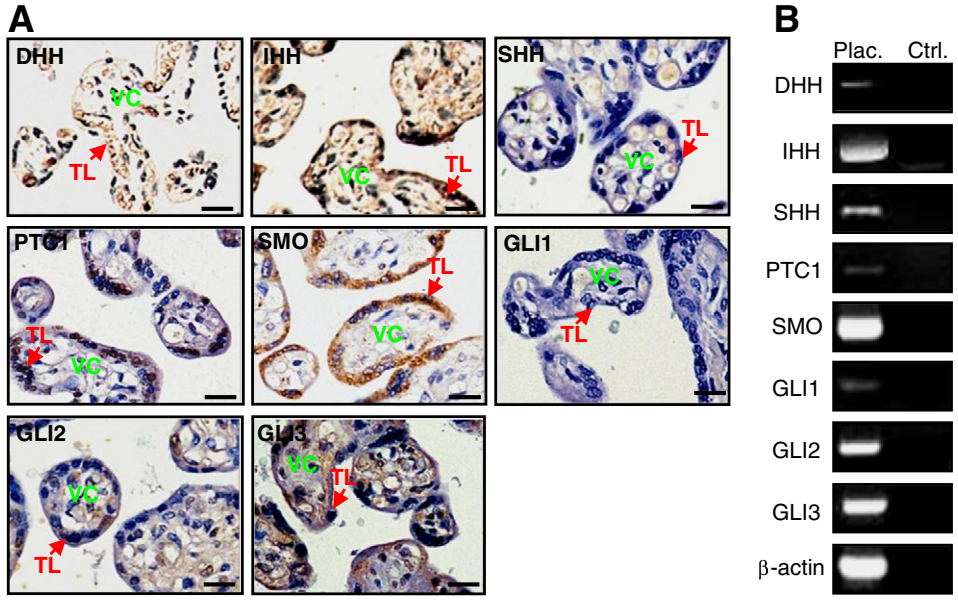

Fig. 1. Expression patterns of main components of HH pathway in human placenta. (A) Immunohistochemistry staining for the main components of HH pathway by using paraffin-embedded sections of human term placentas. (B) RT-PCR assays for mRNA levels of the main components of HH pathway in human term placentas. VC, villous core; TL, trophoblast layer; Plac., placenta; Ctrl., negative control that is absent of cDNA for RT-PCR; bar, 20 μM.

with either GLI antibodies or control IgG. After the immunoprecipitates were incubated with protein A agarose/salmon sperm DNA, the antibody–protein–DNA–agarose complex was washed and harvested for subsequent reverse cross-linking. The sheared DNA fragments from reverse cross-linking were extracted with a DNA extraction kit for further PCR amplification by using the primers listed in the Supplementary data (Table S3).

2.11. Statistical analysis

All the numerous data were expressed as mean ± SD, and were analyzed by one-way ANOVA and Tukey–Kramer multiple comparison test (SPSS 13.0J software; SPSS, Inc., Chicago, IL). Statistical significance was assessed at $p < 0.05$ and $p < 0.01$. Experiments were independently triplicated, and results were qualitatively identical. Representative experiments are shown.

3. Results

3.1. Expression of the main components of HH pathway in human placenta

In human placental villi, the epithelial covering is composed of two distinct layers: the STB layer and the underlying CTB layer, separating the intervillous space from the villous core that consists of mesenchymal connective tissue and fetal blood vessels [18,22]. To examine the expression pattern of HH signaling components, we performed immunohistochemistry of human term placentas. DHH and IHH were robustly expressed in the villous core and the trophoblast layers, respectively, whereas SHH was expressed at low levels in both trophoblast layers and villous cores (Fig. 1A). PTC1 and SMO were predominantly expressed in the trophoblast layers, whereas GLI2 and GLI3, in contrast to GLI1 that was barely detectable, were abundantly distributed in both trophoblast layers and villous cores (Fig. 1A). To gain quantitative information about the expression of HH signaling components, we performed RT-PCR assays. Human term placentas expressed relatively higher levels of IHH, SHH, SMO, GLI2, and GLI3 than DHH, PTC1, and GLI1 (Fig. 1B). Overall, the expression of HH ligands in the villous cores (HH-producing tissues), and PTC1 and SMO in trophoblast layers (HH-responding tissues) suggests that HH signaling may regulate the physiological function of human placental trophoblasts.

3.2. Induction of EMT by HH in cytotrophoblasts

To investigate the potential roles of HH signaling in EMT of cytotrophoblasts, we treated the cells with SHH conditional medium (SM) and control conditional medium (CM) for up to 48 h. SM time-

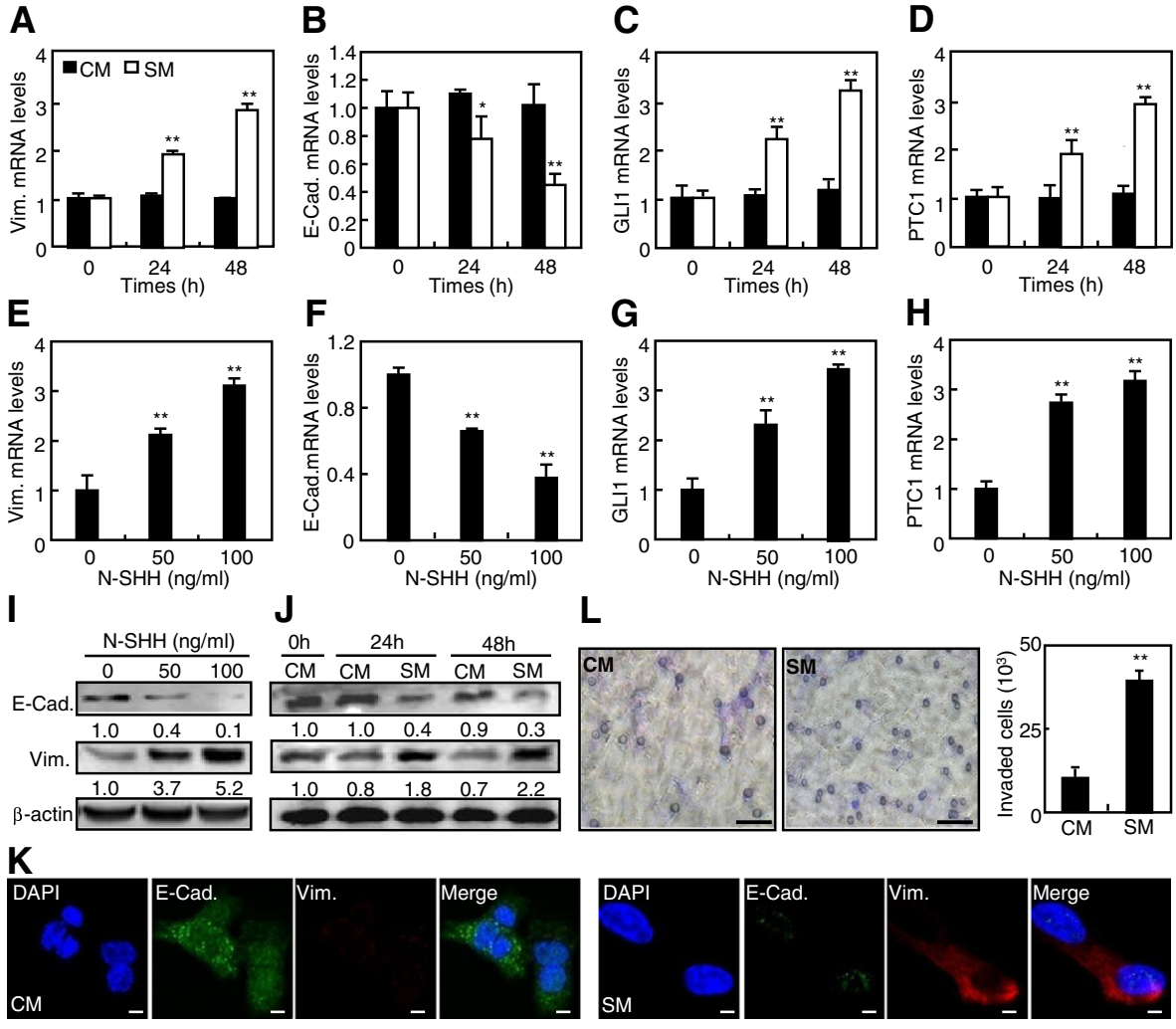

Fig. 2. Induction of EMT by SHH in primary cytotrophoblasts. (A–J) After the cytotrophoblasts treated with either SHH conditional medium (SM) and control conditional medium (CM) for indicated times or the indicated concentrations of SHH (N-SHH) for 48 h, the mRNA and protein levels of vimentin (Vim.) and E-Cadherin (E-Cad.) and the mRNA levels of PTC1 and GLI1 were examined. (K) Immunofluorescent staining of vimentin and E-Cadherin after cells were treated with SM or CM for 48 h. (L) The invasion ability of cells was assessed by Matrigel-coated chamber assay. The relative RNA abundance and protein abundance were normalized to β-actin, respectively. $^{**}p < 0.01$, $^{*}p < 0.05$ versus CM or 0 ng/ml N-SHH, n = 6; bar, 20 μM.

dependently induced both mRNA and protein levels of vimentin (Vim.), a mesenchymal marker, up to 2.8-fold and 3.1-fold, respectively; but decreased them of E-Cadherin (E-Cad.), an epithelial marker, by 56% and 67%, respectively, after 48 h treatment (Fig. 2A, B and J). To confirm the specificity of SM in induction of EMT, we treated cells with different concentrations of biological active SHH recombinant protein (N-SHH). Similarly, N-SHH dose-dependently induced both mRNA and protein levels of vimentin up to 3.2-fold and 5.2-fold, respectively; but decreased them of E-Cadherin by 56% and 67%, respectively, at 100 ng/ml (Fig. 2E, F and I). The specificity of SM was further confirmed by 5E1 SHH blocking antibody, SHH neutralizing antibody at 10 mg/ml almost completely abrogated the SM-induced decreases in E-Cadherin mRNA and increases in vimentin mRNA (Fig. S1A). In the control experiments, SM induced the mRNA levels of PTC1 and GLI1, the target genes of HH signaling, up to 2.9-fold and 3.3-fold, respectively (Fig. 2C and D); whereas SHH recombinant protein at 100 ng/ml induced their mRNA levels up to 3.2-fold and 3.5-fold, respectively (Fig. 2G and H). To examine the intracellular localization and the levels of E-Cadherin and vimentin, we performed the immunofluorescent staining. E-Cadherin was evenly distributed in the cytotrophoblasts, but vimentin was predominantly localized in the cytoplasmic fractions. Treatment with SM robustly enhanced the vimentin-derived immunofluorescent signals, but attenuated E-Cadherin-derived immunofluorescent signals (Fig. 2K). To further determine the mesenchymal phenotypes of cytotrophoblasts after treatment with SM, we assessed the invasion ability of cells by Matrigel-coated chamber assay. SM treatment for 48 h led to an approximately 3.8-fold increase in invasion into the Matrigel as compared to CM treatment (Fig. 2L). Thus, HH ligand stimulates the EMT of human placental cytotrophoblasts.

3.3. Induction of EMT in trophoblast-like JEG-3 cells by HH

Human trophoblast-like cell lines are commonly used as a cell culture model to mimic in vivo biological behavior of placental villous trophoblast [16,17]. Before using human trophoblast-like JEG-3 cells to explore the potential mechanisms responsible for HH-induced EMT in cytotrophoblasts, we further confirmed the effects of HH on EMT in this cell line. Similar to cytotrophoblasts, in JEG-3 cells, SHH time- and dose-dependently induced the expression of vimentin but decreased the expression of E-Cadherin, and JEG-3 cells appeared to be more sensitive than cytotrophoblasts in response to SHH (Fig. 3A and B). The distribution of E-Cadherin in JEG-3 cells was different in cytotrophoblasts, and in JEG-3 cells, E-Cadherin was predominantly localized in the cell membrane fraction, whereas in cytotrophoblasts, it was evenly localized in the cell membrane and cytoplasmic fractions (Fig. 3C). To investigate the transdifferential effect of SHH in JEG-3 cells, we assessed the mesenchymal phenotypes by wound healing, Matrigel invasion and colony formation assays. After 48 h exposure to SM, morphology of JEG-3 cells was changed to a mesenchymal character with an elongated and disseminated appearance, and SM treatment led to approximately 2.1-fold increases in migration of JEG-3 cells in wound healing, 4.3-fold increases in invasion into the Matrigel, and 12-fold increases in colony formation as compared to CM treatment (Fig. 3D–F). Thus, HH ligand stimulates the EMT not only in human primary cytotrophoblasts but also in human trophoblast-like JEG-3 cells.

3.4. Smoothened-dependent induction of EMT by HH

In order to determine whether HH-induced EMT is SMO-dependent or not in JEG-3 cells, we inhibited HH signaling by a SMO inhibitor, cyclopamine, and activated HH signaling by either SMO agonist, purmorphamine, or constitutively active form of SMO (SMO*). Treatment of JEG-3 cells with cyclopamine (Cyc) dose-dependently reversed the increases in vimentin and the decreases in E-Cadherin at both mRNA and protein levels in response to the SHH (Fig. 4A and B). Cyclopamine at 5 μM (Cyc5) attenuated SHH-induced vimentin mRNA and protein levels by 32% and 57%, respectively; and potentiated SHH-negated E-Cadherin mRNA and protein levels up to 2.3- and 8.0-fold, respectively (Fig. 4A). Conversely, activation of SMO by either purmorphamine or overexpression of SMO* significantly increased vimentin and decreased E-Cadherin mRNA and protein levels, and purmorphamine at 2 μM increased vimentin mRNA and protein levels up to 2.9- and 3.2-fold, respectively, and negated E-Cadherin mRNA and protein levels by 55% and 90%, respectively (Fig. 4C and D). SMO* increased vimentin mRNA and protein levels up to 3.5- and 4.4-fold, respectively, and decreased E-Cadherin mRNA and protein levels by 72% and 90%, respectively (Fig. 4F and G). In the control experiments, purmorphamine induced the mRNA levels of PTC1 and GLI1, the target genes of SHH signaling,

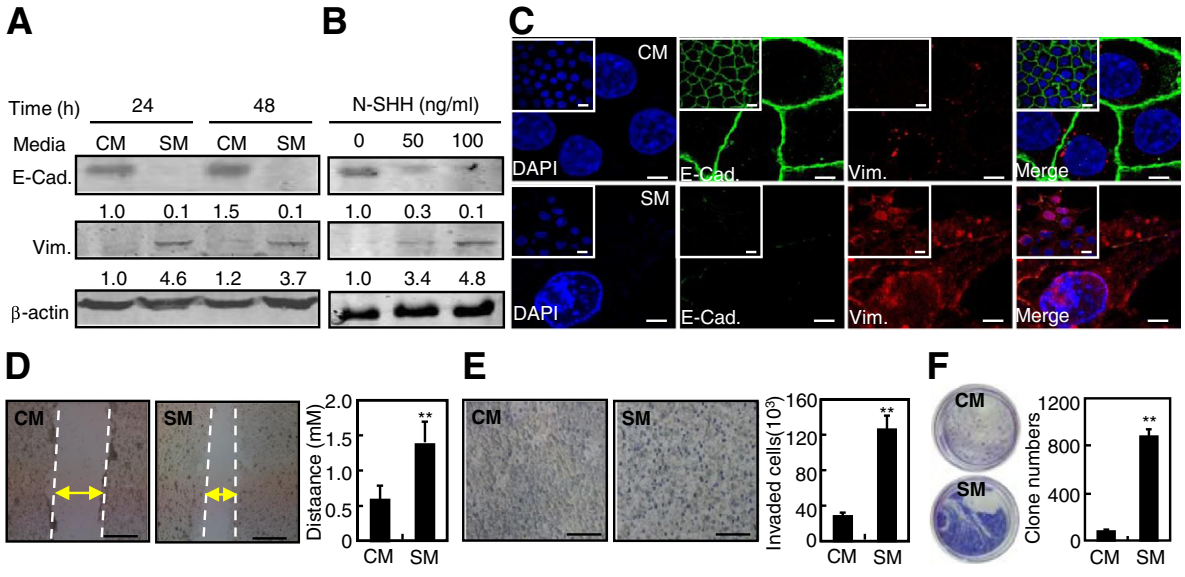

Fig. 3. Induction of EMT in trophoblast-like JEG-3 cells by SHH. (A, B) JEG-3 cells were treated with either SHH conditional medium (SM) and control conditional medium (CM) for indicated times or the indicated concentrations of SHH recombinant protein (N-SHH) for 48 h, then, the protein levels of vimentin (Vim.) and E-Cadherin (E-Cad.) were examined. (C) Immunofluorescent staining of vimentin and E-Cadherin after cells were treated with SM or CM for 48 h. (D–F) Wound healing, Matrigel invasion and colony formation assays were used to assess the mesenchymal phenotypes of JEG-3 cells. Protein abundance was normalized to β-actin. $^{**}p < 0.01$ versus CM, n = 6; bar, 20 μM.

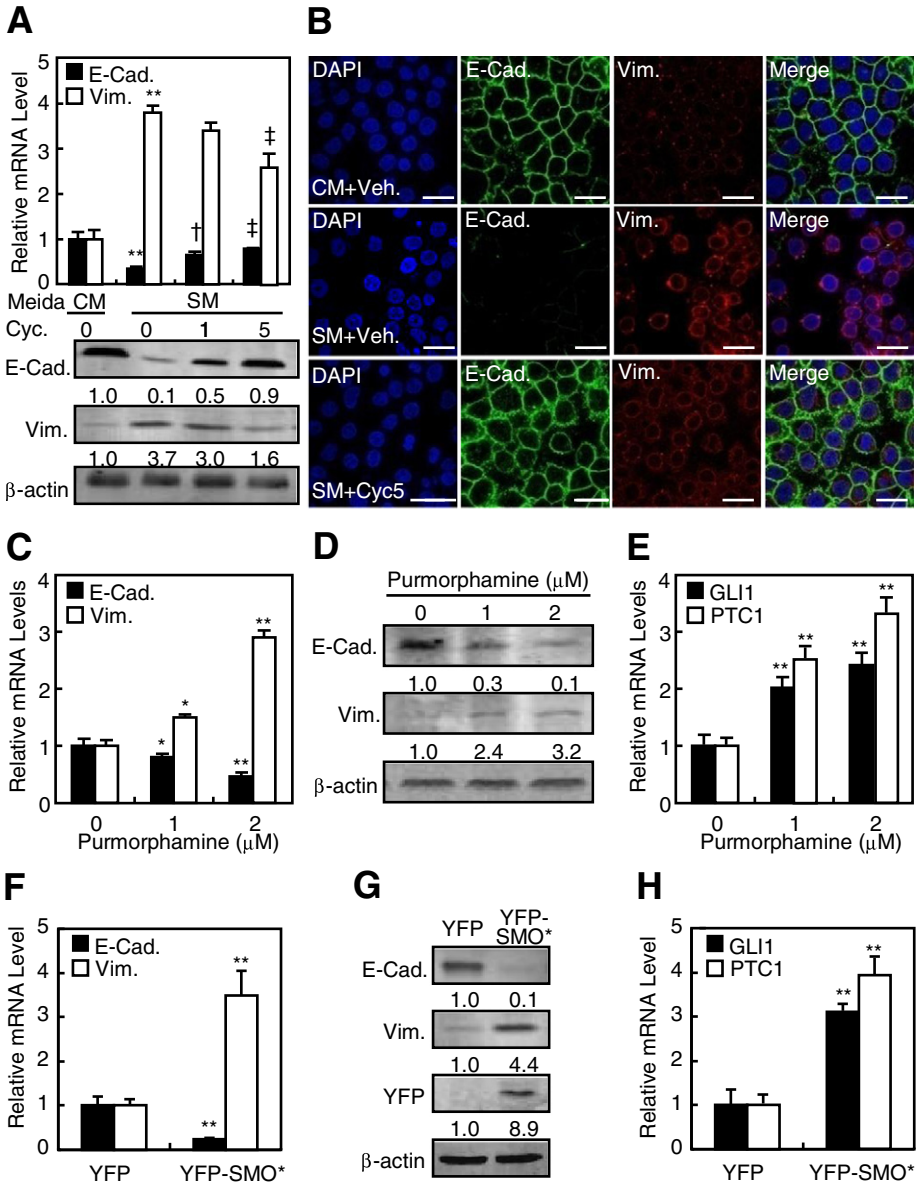

Fig. 4. Smoothened (SMO)-dependent induction of EMT by HH. (A, B) JEG-3 cells were treated with the indicated concentrations of cyclopamine (Cyc) in the presence of CM or SM for 48 h, then the mRNA and protein levels of vimentin (Vim.) and E-Cadherin (E-Cad.) were examined. (C–E) JEG-3 cells were treated with the indicated concentrations of purmorphamine for 48 h, then the mRNA and protein levels of vimentin and E-Cadherin and the mRNA levels of GLI1 and PTC1 were examined. (F–H) After retroviral overexpression of constitutively active form of SMO (SMO*) in JEG-3 cells for 48 h, the mRNA and protein levels of vimentin and E-Cadherin and the mRNA levels of GLI1 and PTC1 were examined. RNA abundance and protein abundance were normalized to β-actin, respectively. $^{**}p < 0.01$, $^{*}p < 0.05$ versus CM without cyclopamine, 0 μM purmorphamine or YFP; $^{‡}p < 0.01$, $^{†}p < 0.05$ versus SM without cyclopamine; n = 6; bar, 20 μm.

up to 3.4-fold and 2.4-fold, respectively (Fig. 4E); whereas SMO* induced their mRNA levels up to 4.0-fold and 3.2-fold, respectively (Fig. 4H). Thus, HH-induced EMT is SMO-dependent, and activation of SMO alone is sufficient to induce the EMT in JEG-3 cells.

3.5. Distinct roles of GLI transcriptional factors in HH-induced EMT

In order to assess the potential involvement of GLI transcriptional factors in the HH-induced EMT, we generated lentiviruses expressing GLI1–, GLI2–, or GLI3–shRNA which knocked down the expression of GLI1, GLI2, and GLI3 by as much as 55–80% at either mRNA or protein levels (Fig. 5A–C). Knockdown of GLI1 reversed SHH-negated E-Cadherin mRNA levels by 2.8-fold and protein levels by 3.0-fold (Fig. 5D and E), and attenuated SHH-induced vimentin mRNA levels by 33% and protein levels by 75% (Fig. 5D and F). On the other hand, knockdown of GLI2 increased SHH-negated E-Cadherin mRNA levels by 3.3-fold and protein levels by 2.5-fold (Fig. 5D and E), and attenuated SHH-induced vimentin mRNA levels by 48% and protein levels by 72% (Fig. 5D and F). However, knockdown of GLI3 affected neither the SHH-negated E-Cadherin mRNA and protein levels, nor SHH-induced vimentin mRNA and protein levels (Fig. 5D–F). Conversely, overexpression of GLI1 suppressed the mRNA levels of E-Cadherin by 60% and protein level by 50%, and induced the mRNA levels of vimentin by 3.8-fold and protein levels by 5-fold (Figs. 5G and S1B). Overexpression of ΔN-GLI2 suppressed the mRNA expression of E-Cadherin by 70% and protein level by 80%, and induced the mRNA expression of vimentin by 4.2-fold and protein level by 5.2-fold (Figs. 5H and S1B). However, over-expression of GLI3 affected neither the E-Cadherin nor vimentin mRNA levels (Fig. 5I). In wound healing, knockdown of GLI1 and GLI2 but not GLI3 attenuated SHH-induced cell migration by 56% and 57%, respectively (Figs. 5J and S1C). In Matrigel invasion, knockdown of GLI1 and GLI2 but not GLI3 attenuated SHH-induced cell invasion by

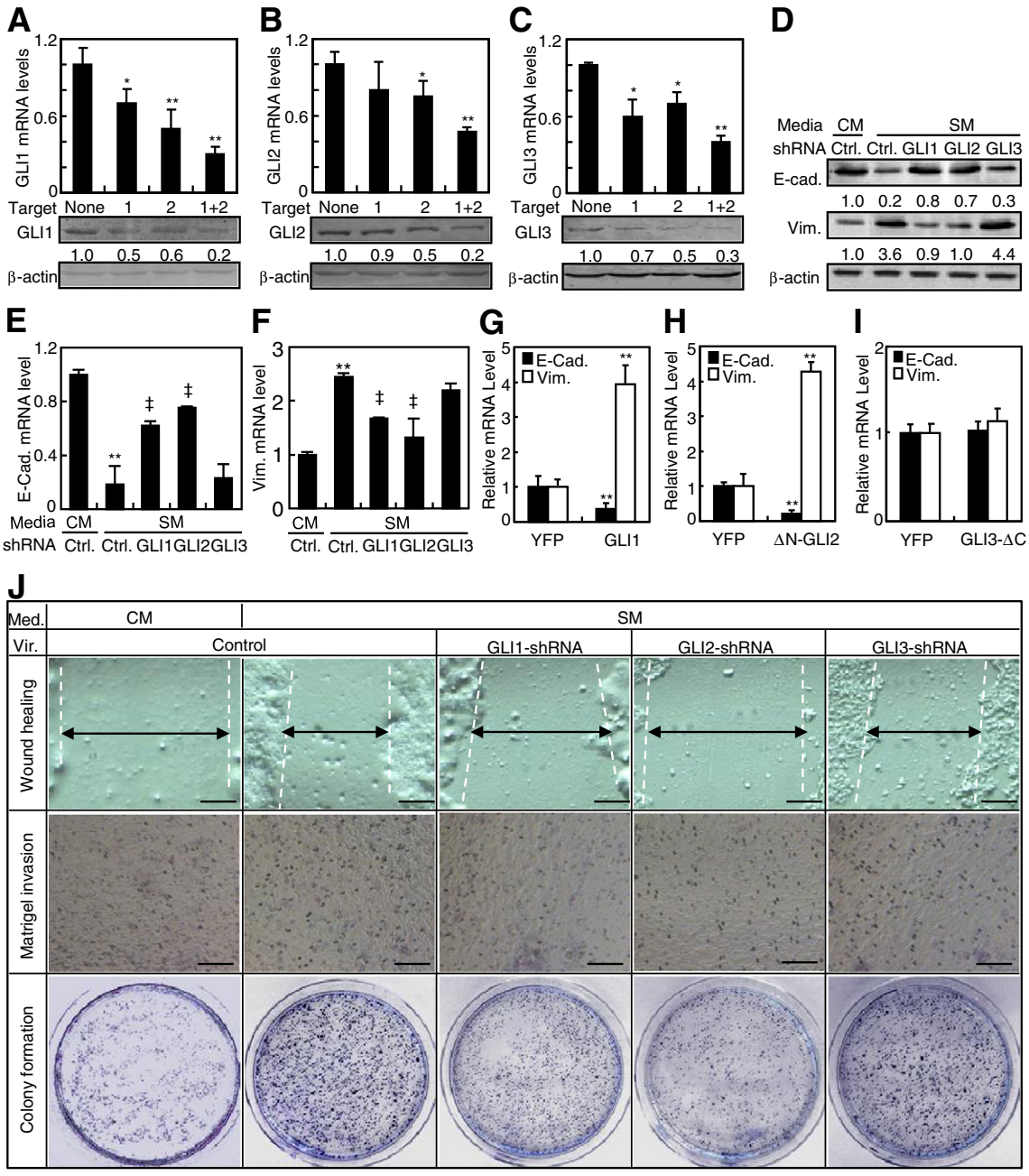

Fig. 5. Distinct roles of GLI transcriptional factors in HH-induced EMT. (A–C) Knockdown efficiencies of GLI1–, GLI2–, or GLI3–shRNA-expressing lentiviruses were examined by quantitative real-time PCR and Western blotting. (D–F) The mRNA and protein levels of E-Cadherin and vimentin were examined after GLIs were knocked down in JEG-3 cells in the presence of CM or SM. (G–I) The mRNA levels of E-Cadherin and vimentin were examined in JEG-3 cells infected with retroviruses expressing GLI1, active form of GLI2 (ΔN-GLI2) or GLI3 repressor (GLI3-ΔC), respectively. (J) Wound healing, Matrigel invasion and colony formation assays were performed to assess the mesenchymal phenotypes of JEG-3 cells after GLIs were knocked down in the presence of SM. RNA abundance and protein abundance were normalized to β-actin, respectively. $^{**}p < 0.01$, $^{*}p < 0.05$ versus None, CM with control shRNA, or vector; $^{‡}p < 0.01$, $^{†}p < 0.05$ versus SM with control shRNA; n = 6; bar, 50 μm.

54% and 44%, respectively (Figs. 5J and S1D). Similarly, knockdown of GLI1 and GLI2 but not GLI3 attenuated SHH-induced colony formation by 45% and 32%, respectively (Figs. 5J and S1E). Thus, both GLI1 and GLI2 mediate HH-induced changes of epithelial phenotypes to mesenchymal phenotypes in JEG-3 cells. To further confirm the roles of GLI1 and GLI2, we manipulated rescue experiments. As a result, over-expression of GLI1 was able to rescue the GLI1 knockdown-resulted changes in mRNA expression of E-Cadherin and vimentin, and in wound healing (Fig. S2A–C). And over-expression of GLI2 was also able to rescue the GLI2 knockdown-resulted changes in mRNA expression of E-Cadherin and vimentin, and in wound healing (Fig. S2A–C).

3.6. HH-induced expression of key transcriptional factors of EMT through GLI1

The changes in gene expression that contribute to the repression of the epithelial phenotype and activation of the mesenchymal phenotype involve master regulators, including Snail, Twist and zinc-finger E-box-binding (ZEB) transcription factors [5]. To investigate the effects of HH on these transcriptional factors, we performed quantitative RT-PCR to determine the mRNA levels of Slug (sanil2), Snail (sanil1) and Twist. In JEG-3 cells, SHH significantly induced the mRNA levels of Slug, Snail, Twist as well as GLI1, the HH's target gene, up to 2.3-, 2.6-, 2.8-,

and 3.3-fold respectively; however, knockdown of GLI1 but not GLI2 and GLI3 decreased SHH-induced mRNA levels by 40%, 50%, 36%, and 61%, respectively (Fig. 6A–C). Thus, GLI1-controlled Slug, Twist and Snail transcription might contribute to the HH-induced EMT in JEG-3 cells.

3.7. CDH1 as a direct downstream target gene of both GLI1 and GLI2

GLI2 is not responsible for the HH-induced expression of key transcriptional factors of EMT. To investigate whether *CDH1* gene encoding E-Cadherin and *VIM* gene encoding vimentin are direct transcriptional

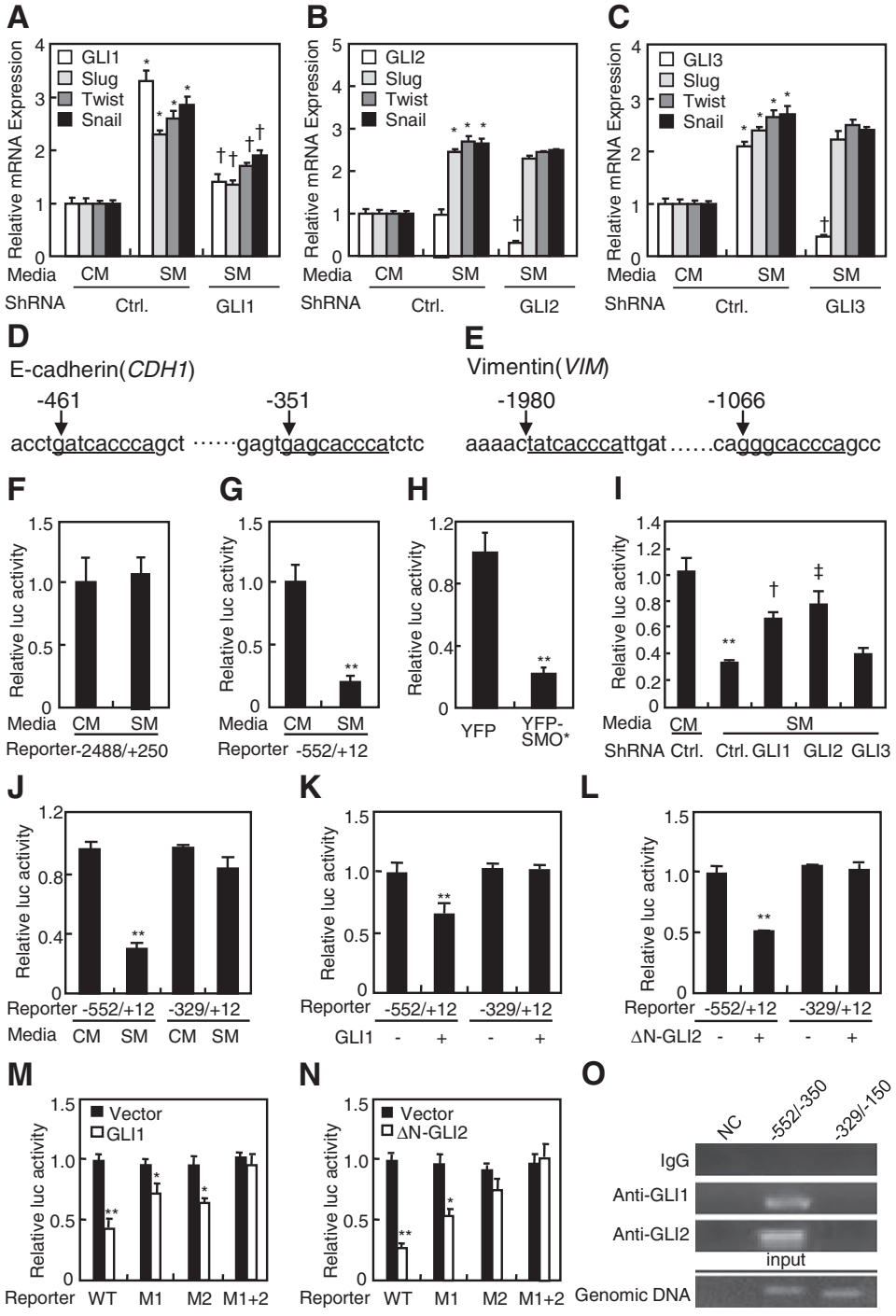

Fig. 6. E-Cadherin as a direct downstream target gene of both GLI1 and GLI2. (A–C) The mRNA levels of Slug (sanil2), Snail (sanil1) and Twist were determined by quantitative RT-PCR in JEG-3 cells infected with GLIs–shRNA-expressing lentiviruses for 48 h in the presence of CM or SM. (D, E) Schematic presentations of promoter regions with potential GLI consensus and non-consensus binding sites of *CDH1* and *VIM* genes encoding E-Cadherin and vimentin, respectively. (F) Dual-luciferase assays in JEG-3 cells after transient transfection with reporter constructs of *VIM* and treatment with CM or SM for 48 h. (G–I) Dual-luciferase assays of *CDH1* reporter in JEG-3 cells after treatment with CM or SM, infection with retroviruses expressing YFP or YFP-SMO*, or lentiviruses expressing GLIs–shRNA in the presence of CM or SM for 48 h. (J–L) Dual-luciferase assays in JEG-3 cells after transfection with delete mutants of *CDH1* reporter and treatment with CM and SM or co-transfection with delete mutant and active form of GLIs for 48 h. (M, N) Dual-luciferase assays after transient co-transfection with active form of GLIs and *CDH1* reporter variants (WT, wild type) that harbored mutations at individual (M1 or M2) or double (M1 + 2) GLI response elements. (O) Chromatin immunoprecipitation followed by PCR (ChIP-PCR) in JEG-3 cells by using antibodies against GLI1 and GLI2. The abundance was normalized to the corresponding input. $^{**}p < 0.01$, $^{*}p < 0.05$ versus CM with control shRNA; $^{\ddagger}p < 0.01$, $^{\dagger}p < 0.05$ versus SM with control shRNA; n = 6.

targets of GLI2 in response to SHH, we cloned the promoter regions (nt −552/+12 for *CDH1* and nt −2488/+250 for *VIM*) containing the consensus and non-consensus GLI response elements (GRE) (Fig. 6D and E, underline), and generated luciferase reporter constructs and their mutants. Though SHH did not induce the luciferase activities of *VIM* reporter (Fig. 6F), either SHH treatment or over-expression of SMO* significantly negated *CDH1* reporter activities (Fig. 6G and H). Conversely, knockdown of either GLI1 or GLI2 but not GLI3 significantly reversed SHH-negated luciferase activities of *CDH1* (Fig. 6I), and deletion of nt −552/−330 almost completely abolished SHH-, GLI1- or ΔN-GLI2-negated *CDH1* luciferase activities (Fig. 6J–L). To further examine the functionality of GLI consensus and non-consensus binding sites, we generated *CDH1* (nt −552/+12) reporter variants that harbored mutations at individual (M1 or M2) or double (M1 + 2) GRE. Each individual GRE mutation significantly attenuated the response to either GLI1 or ΔN-GLI2, whereas the double mutations virtually abolished the response altogether (Fig. 6M and N). To examine the physical interaction between GLIs and the promoter regions of *CDH1* genes, we performed chromatin immunoprecipitation followed by PCR (ChIP-PCR) in JEG-3 cells by using antibodies against GLI1 and GLI2. The PCR primers were designed to amplify specific genomic DNA fragments of nt −552/−350 and nt −329/−150 for *CDH1*. And the ChIP assays were normalized to their corresponding input. GLI2 robustly bound to the fragment of nt −552/−350 but not nt −329/−150, and GLI1 also bound to the fragment of nt −552/−350 but not nt −329/−150 either (Fig. 6O). Thus, we have identified *CDH1* as a direct downstream target gene of HH signaling.

4. Discussion

The present study describes, to our knowledge for the first time, the roles and underlying mechanisms of HH signaling in human placental EMT. At the molecular level, HH induces the transcription of key EMT regulators including Snail1, Slug, and Twist through GLI1, and negatively regulates the downstream target gene, *CDH1* encoding E-Cadherin, through both GLI1 and GLI2. Our results therefore identify HH as critical signals in supporting the physiological function of mature placenta.

The tissue-specific HH ligands are secreted by HH-producing cells, and act upon the HH-responding cells to fulfill the signaling transduction [24]. We suggest that HH proteins may signal through both autocrine and paracrine mechanisms to regulate EMT of placental trophoblasts. Although the present work deals only with EMT by the trophoblasts, HH can act on the stromal cells in villous core to produce the various connective tissue fibers and increase the mechanical stability [25]. Our finding expands the list of tissues and cells influenced by HH signaling. Beyond the critical roles of HH signaling in EMT of human trophoblasts as reported here, HH signaling has been implicated in EMT in many pathological conditions. These include the progression of pancreatic carcinoma, gastrointestinal neuroendocrine tumors, hepatocellular carcinoma, lung squamous cell carcinoma, and liver and kidney fibrosis [11–15,26]. In the current study, we identified that GLI1 mediates HH-induced EMT through upregulation of key EMT regulator including Slug, Snail1, and Twist, this finding is consistent with the previous reporters that GLI1 promotes EMT through its binding to the promoter region of Slug, Snail and Twist and induction of their expression in cancer cells [27,28], and that GLI1 induced an EMT in rat kidney epithelial cells via induction of the E-Cadherin repressor Snail [15]. Upregulation of these EMT regulators is associated with more malignant phenotypes in a variety of human cancer, such as gastric cancer, pancreatic cancer, breast cancer, and ovarian cancer [29], and downregulation of these EMT regulators correlates to the preeclampsia in pregnancy [30–33]. Moreover, in the present study, we also identified that GLI1 acts as a novel transcriptional repressor of *CDH1* gene that encodes E-Cadherin. Our findings correspond to the previous finding that established *CDH1* as a novel transcriptional target of GLI1 in pancreatic ductal adenocarcinoma, and that knockdown of GLI1 abolished characteristics of epithelial differentiation, increased cell motility whereas this effect of GLI1 is fulfilled not through the induction of Snail or Slug but its direct regulation of the transcription of E-Cadherin [34]. Though GLI1 is generally accepted as a transcriptional activator, it is likely that GLI1 recruits some repressive co-factor to form the transcriptional complex in the promoter region of *CDH1* gene, and consequently suppresses the transcription of *CDH1* gene. Alternatively, given the fact that the promoter region of *CDH1* is rich of CpGs islands, we speculate that GLI1-mediated methylation of *CDH1* gene promoter could be the underlying epigenetic mechanisms that contribute to GLI1-negated *CDH1* transcription. Finally, genome-wide screening revealed that SHH/GLI1 signal targeted to an EMT molecular network consisting of TGF-β, Ras, Wnt, growth factors, PI3K/AKT, integrins, transmembrane 4 superfamily (TM4SF), and S100A4 signals to promote EMT in pancreatic cancer cells [35].

Unexpectedly, our finding has uncovered a hitherto uncharacterized role of GLI2 in transactivation of *CDH1* gene. Although GLI2 unlike GLI1 is not responsible for the expression of key EMT regulator including Snail, Slug, and Twist, the Chip-PCR assays revealed that GLI2 binds more than GLI1 to the promoter region of *CDH1* gene encoding the E-Cadherin. E-Cadherin is important for maintaining cell attachment and the layered phenotype of the villous cytotrophoblast, and reduced expression and re-organization of E-Cadherins from cell junctional regions promote a loosened connection between cells, coupled with reduced apico-basal polarity. E-Cadherin is well placed to be key regulators of trophoblast cell behavior, analogous to their role in other developmental EMT [36]. Although GLI2 has been established as a key regulator coupled with TGF-β signaling in the invasion of melanoma, GLI2-mediated invasion of cancer cells is not HH signaling-dependent but TGF-β signaling dependent effects, suggesting that non-canonical HH signaling is involved in the EMT of melanoma [37,38]. GLI1 is responsible for the HH-induced expression of key EMT regulators, resulting in concomitant upregulation of vimentin, GLI2 also mediates HH-induced vimentin expression, whereas GLI2 neither directly transactivates the vimentin gene, nor affected the expression of key EMT regulators, thus, we suppose that there are other mechanisms governing GLI2-mediated EMT, and further experiments need to be set up to address this issue.

Human trophoblast-like cell lines are commonly used as cell culture models to mimic in vivo biological behavior of placental villous trophoblast [16,17], though human primary cytotrophoblasts behave differently from trophoblast-like cells in some aspects. Since EMT JEG-3 cells function in a similar way to primary cytotrophoblasts in response to HH, we suggest that the findings derived from the cell line could be transferable to the primary cells. Two very different but clinically relevant pregnancy disorders characteristically present with shallow trophoblast invasion into the maternal environment. These are fetal growth restriction (FGR) and pre-eclampsia (PE) [8,31–33]. Although several factors may influence both PE and FGR, placental factors, specifically, insufficient trophoblast differentiation and invasion, may contribute to these serious pregnancy disorders [39,40]. The growth, migration and invasion of placental cells into the uterine milieu are relevant to the initial establishment of a healthy pregnancy, and are compromised in both FGR and PE. In addition, since these same processes are continual in normal placental development, placental growth, migration and invasion in later stage pregnancies are also critical [8,41,42]. Given the malformation of the placenta is an underlying feature of a great variety of human developmental abnormalities and pregnancy-associated diseases, the identification of HH signaling critical for the EMT in human placenta may help pinpoint the underlying mechanisms involved in the etiology of these conditions.

In summary, the present study has shown that HH pathway is essential for trophoblastic EMT, a critical process for placentation. In this molecular event, both Gil1 and GLI2 function as direct transcriptional repressor of *CDH1* gene encoding E-Cadherin, and GLI1 alone is responsible for the HH-induced transcription of key EMT regulators including

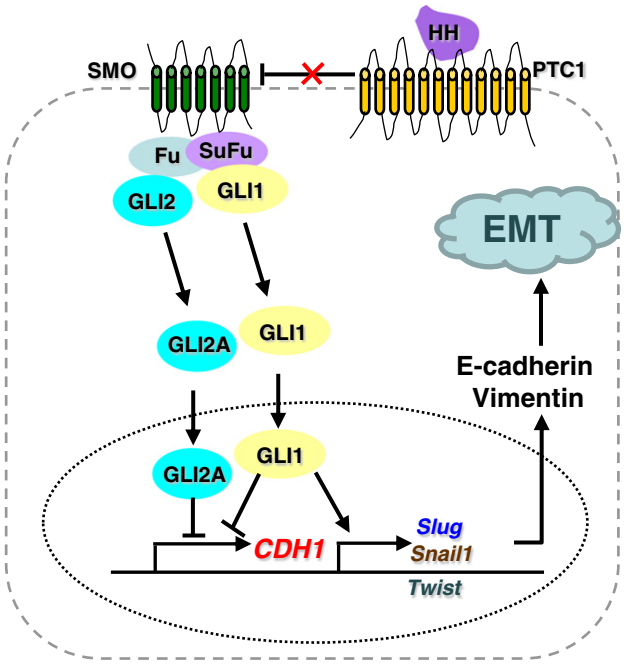

Fig. 7. Schematic graph showing the proposed model for HH-induced EMT in human trophoblasts. In the presence of HH, binding of HH to PTC1 relieves the inhibition of SMO, resulting in activation of GLI1 and GLI2. Activation of both GLI1 and GLI2 negates the transcription of their down-stream target gene, *CDH1* encoding E-Cadherin, and activation of GLI1 simultaneously promotes the transcription of key EMT regulators including Slug, Snail1, and Twist. As a result, up-regulation of key EMT regulators and down-regulation of E-Cadherin expression induce the transdifferentiation of human trophoblasts from epithelial to mesenchymal phenotype.

Snail1, Slug, and Twist (Fig. 7). Thus, HH through GLI1 and GLI2 acts as critical signals in supporting the physiological function of the placenta.

Disclosure summary

The authors have nothing to disclose.

Transparency document

The Transparency document associated with this article can be found in the online version.

Acknowledgements

We thank Dr. Sasaki for his generous donation of plasmid and Dr. Fanxin Long from Washington University in St. Louis for his advice and comments on this work. This work is supported by 973 Program (no. 2011CB944403), National Natural Science Foundation of China (no. 30973580, no. 31071292, no. 81370713), and Natural Science Foundation of Zhejiang Province, China (no. R2110269).

Appendix A. Supplementary data

Supplementary data to this article can be found online at http://dx.doi.org/10.1016/j.bbagen.2015.04.005.

References

[1] Y. Chen, G. Struhl, Dual roles for patched in sequestering and transducing Hedgehog, Cell 87 (1996) 553–563.
[2] P.W. Ingham, A.P. McMahon, Hedgehog signaling in animal development: paradigms and principles, Genes Dev. 15 (2001) 3059–3087.
[3] D.J. Robbins, D.L. Fei, N.A. Riobo, The hedgehog signal transduction network, Sci. Signal. 5 (2012) re6.
[4] M. Varjosalo, J. Taipale, Hedgehog: functions and mechanisms, Genes Dev. 22 (2008) 2454–2472.
[5] S. Lamouille, J. Xu, R. Derynck, Molecular mechanisms of epithelial–mesenchymal transition, Nat. Rev. Mol. Cell Biol. 15 (3) (2014) 178–196.
[6] A. Puisieux, T. Brabletz, J. Caramel, Oncogenic roles of EMT-inducing transcription factors, Nat. Cell Biol. 16 (6) (2014) 488–494.
[7] T.M. Mayhew, Turnover of human villous trophoblast in normal pregnancy: what do we know and what do we need to know? Placenta 35 (4) (2014) 229–240.
[8] M.I. Kokkinos, P. Murthi, R. Wafai, E.W. Thompson, D.F. Newgreen, Cadherins in the human placenta–epithelial–mesenchymal transition (EMT) and placental development, Placenta 31 (9) (2010) 747–755.
[9] A.E. Wallace, R. Fraser, J.E. Cartwright, Extravillous trophoblast and decidual natural killer cells: a remodelling partnership, Hum. Reprod. Update 18 (4) (2012) 458–471.
[10] A. Jurisicova, J. Detmar, I. Caniggia, Molecular mechanisms of trophoblast survival: from implantation to birth, Birth Defects Res. C Embryo Today 75 (4) (2005) 262–280.
[11] D. Yue, H. Li, J. Che, Y. Zhang, H.H. Tseng, J.Q. Jin, T.M. Luh, E. Giroux-Leprieur, M. Mo, Q. Zheng, H. Shi, H. Zhang, X. Hao, C. Wang, D.M. Jablons, B. He, Hedgehog/Gli promotes epithelial–mesenchymal transition in lung squamous cell carcinomas, J. Exp. Clin. Cancer Res. 33 (2014) 34.
[12] J.S. Chen, H.S. Li, J.Q. Huang, L.J. Zhang, X.L. Chen, Q. Wang, J. Lei, J.T. Feng, Q. Liu, X.H. Huang, Down-regulation of Gli-1 inhibits hepatocellular carcinoma cell migration and invasion, Mol. Cell. Biochem. 393 (1–2) (2014) 283–291.
[13] K.D. Marini, B.J. Payne, D.N. Watkins, L.G. Martelotto, Mechanisms of Hedgehog signalling in cancer, Growth Factors 29 (6) (2011) 221–234.
[14] A. Omenetti, A. Porrello, Y. Jung, L. Yang, Y. Popov, S.S. Choi, R.P. Witek, G. Alpini, J. Venter, H.M. Vandongen, W.K. Syn, G.S. Baroni, A. Benedetti, D. Schuppan, A.M. Diehl, Hedgehog signaling regulates epithelial–mesenchymal transition during biliary fibrosis in rodents and humans, J. Clin. Invest. 118 (10) (2008) 3331–3342.
[15] H. Ding, D. Zhou, S. Hao, L. Zhou, W. He, J. Nie, F.F. Hou, Y. Liu, Sonic hedgehog signaling mediates epithelial–mesenchymal communication and promotes renal fibrosis, J. Am. Soc. Nephrol. 23 (5) (2012) 801–813.
[16] X. Wu, T. Iguchi, N. Itoh, K. Okamoto, T. Takagi, K. Tanaka, T. Nakanishi, Ascorbic acid transported by sodium-dependent vitamin C transporter 2 stimulates steroidogenesis in human choriocarcinoma cells, Endocrinology 149 (2008) 73–83.
[17] L. Chen, H. Zhu, Y. Pan, C. Tang, M. Watanabe, H. Ruan, Y. Wang, J. Wang, H.Y. Yao, T. Iguchi, X. Wu, Ascorbic acid uptaken by sodium-dependent vitamin C transporter 2 induces βhCG expression through Sp1 and TFAP2A transcription factors in human choriocarcinoma cells, J. Clin. Endocrinol. Metab. 97 (2012) E1667–E1676.
[18] C. Tang, Y. Pan, H. Luo, W. Xiong, H. Zhu, H. Ruan, J. Wang, C. Zou, L. Tang, T. Iguchi, F. Long, X. Wu, Hedgehog signaling stimulates the conversion of cholesterol to steroids, Cell Signal. (Jan 10 2015), http://dx.doi.org/10.1016/j.cellsig.2015.01.004 (pii: S0898-6568(15)00006-6. Epub ahead of print).
[19] R. Favaro, M. Valotta, A.L. Ferri, E. Latorre, J. Mariani, C. Giachino, C. Lancini, V. Tosetti, S. Ottolenghi, V. Taylor, S.K. Nicolis, Hippocampal development and neural stem cell maintenance require Sox2-dependent regulation of SHH, Nat. Neurosci. 12 (2009) 1248–1256.
[20] X. Wu, L.H. Zeng, T. Taniguchi, Q.M. Xie, Activation of PKA and phosphorylation of sodium-dependent vitamin C transporter 2 by prostaglandin E2 promote osteoblast-like differentiation in MC3T3-E1 cells, Cell Death Differ. 14 (2007) 1792–1801.
[21] Y. Wang, C. Tang, M. Wu, Y. Pan, H. Ruan, L. Chen, H. Yao, H. Zhu, X. Wu, Dehydroascorbic acid taken up by glucose transporters stimulates estradiol production through inhibition of JNK/c-Jun/AP1 signaling in JAR cells, Mol. Hum. Reprod. 20 (8) (2014) 799–809.
[22] K.J. Livak, T.D. Schmittgen, Analysis of relative gene expression data using real-time quantitative PCR and the 2(−Delta Delta C(T)) Method, Methods 25 (4) (2001) 402–408.
[23] M.I. Khan, V.M. Adhami, R.K. Lall, M. Sechi, D.C. Joshi, O.M. Haidar, D.N. Syed, I.A. Siddiqui, S.Y. Chiu, H. Mukhtar, YB-1 expression promotes epithelial-to-mesenchymal transition in prostate cancer that is inhibited by a small molecule fisetin, Oncotarget 5 (9) (2014) 2462–2474.
[24] J.N. Li, Y.C. Ge, Z. Yang, C.M. Guo, T. Duan, L. Myatt, H. Guan, K. Yang, K. Sun, The Sp1 transcription factor is crucial for the expression of 11β-hydroxysteroid dehydrogenase type 2 in human placental trophoblasts, J. Clin. Endocrinol. Metab. 96 (2011) E899–E907.
[25] C.J. Huang, H.H. Yao, Diverse functions of hedgehog signaling in formation and physiology of steroidogenic organs, Mol. Reprod. Dev. 77 (2010) 489–496.
[26] V. Meraviglia, M. Vecellio, A. Grasselli, M. Baccarin, A. Farsetti, M.C. Capogrossi, G. Pompilio, D.A. Coviello, C. Gaetano, M. Di Segni, Human chorionic villus mesenchymal stromal cells reveal strong endothelial conversion properties, Differentiation 83 (2012) 260–270.
[27] T. Shida, M. Furuya, T. Nikaido, M. Hasegawa, K. Koda, K. Oda, M. Miyazaki, T. Kishimoto, Y. Nakatani, H. Ishikura, Sonic Hedgehog–Gli1 signaling pathway might become an effective therapeutic target in gastrointestinal neuroendocrine carcinomas, Cancer Biol. Ther. 5 (11) (2006) 1530–1538.
[28] X. Li, W. Deng, S.M. Lobo-Ruppert, J.M. Ruppert, Gli1 acts through Snail and E-Cadherin to promote nuclear signaling by beta-catenin, Oncogene 26 (31) (2007) 4489–4498.
[29] S. Min, X. Xiaoyan, P. Fanghui, W. Yamei, Y. Xiaoli, W. Feng, The glioma-associated oncogene homolog 1 promotes epithelial–mesenchymal transition in human esophageal squamous cell cancer by inhibiting E-Cadherin via Snail, Cancer Gene Ther. 20 (7) (2013) 379–385.
[30] R. Kalluri, EMT: when epithelial cells decide to become mesenchymal-like cells, J. Clin. Invest. 119 (6) (2009) 1417–1419.
[31] A.N. Abell, N.V. Jordan, W. Huang, A. Prat, A.A. Midland, N.L. Johnson, D.A. Granger, P.A. Mieczkowski, C.M. Perou, S.M. Gomez, L. Li, G.L. Johnson, MAP3K4/CBP-regulated H2B acetylation controls epithelial–mesenchymal transition in trophoblast stem cells, Cell Stem Cell 8 (5) (2011) 525–537.

[32] K. Blechschmidt, I. Mylonas, D. Mayr, B. Schiessl, S. Schulze, K.F. Becker, U. Jeschke, Expression of E-Cadherin and its repressor snail in placental tissue of normal, preeclamptic and HELLP pregnancies, Virchows Arch. 450 (2) (2007) 195–202.
[33] Y.Y. Sun, M. Lu, X.W. Xi, Q.Q. Qiao, L.L. Chen, X.M. Xu, Y.J. Feng, Regulation of epithelial–mesenchymal transition by homeobox gene DLX4 in JEG-3 trophoblast cells: a role in preeclampsia, Reprod. Sci. 18 (11) (2011) 1138–1145.
[34] L. Fedorova, C. Gatto-Weis, S. Smaili, N. Khurshid, J.I. Shapiro, D. Malhotra, T. Horrigan, Down-regulation of the transcription factor snail in the placentas of patients with preeclampsia and in a rat model of preeclampsia, Reprod. Biol. Endocrinol. 10 (2012) 15.
[35] S. Joost, L.L. Almada, V. Rohnalter, P.S. Holz, A.M. Vrabel, M.G. Fernandez-Barrena, R.R. McWilliams, M. Krause, M.E. Fernandez-Zapico, M. Lauth, GLI1 inhibition promotes epithelial-to-mesenchymal transition in pancreatic cancer cells, Cancer Res. 72 (1) (2012) 88–99.
[36] X. Xu, Y. Zhou, C. Xie, S.M. Wei, H. Gan, S. He, F. Wang, L. Xu, J. Lu, W. Dai, L. He, P. Chen, X. Wang, C. Guo, Genome-wide screening reveals an EMT molecular network mediated by Sonic hedgehog-Gli1 signaling in pancreatic cancer cells, PLoS One 7 (8) (2012) e43119.
[37] Y. Nakaya, G. Sheng, EMT in developmental morphogenesis, Cancer Lett. 341 (1) (2013) 9–15.
[38] D. Javelaud, M.J. Pierrat, A. Mauviel, Crosstalk between TGF-β and hedgehog signaling in cancer, FEBS Lett. 586 (14) (2012) 2016–2025.
[39] Y. Katoh, M. Katoh, Hedgehog signaling, epithelial-to-mesenchymal transition and miRNA (review), Int. J. Mol. Med. 22 (3) (2008) 271–275.
[40] T. Khong, F. De Wolf, W. Robertson, I. Brosens, Inadequate maternal vascular response to placentation in pregnancies complicated by pre-eclampsia and by small-for-gestational age infants, Br. J. Obstet. Gynaecol. 93 (1986) 1049e59.
[41] K.H. Lim, Y. Zhou, M. Janatpour, M. McMaster, K. Bass, S. Chun, et al., Human cytotrophoblast differentiation/invasion is abnormal in pre-eclampsia, Am. J. Pathol. (1997) 151e6.
[42] W. Li, D. Liu, W. Chang, X. Lu, Y.L. Wang, H. Wang, C. Zhu, H.Y. Lin, Y. Zhang, J. Zhou, H. Wang, Role of IGF2BP3 in trophoblast cell invasion and migration, Cell Death Dis. 5 (2014) e1025.